

# On the Asymptotic MSE-Optimality of Parametric Bayesian Channel Estimation in mmWave Systems

Franz Weißer, *Graduate Student Member, IEEE*, and Wolfgang Utschick, *Fellow, IEEE*

**Abstract**—The mean square error (MSE)-optimal estimator is known to be the conditional mean estimator (CME). This paper introduces a parametric channel estimation technique based on Bayesian estimation. This technique uses the estimated channel parameters to parameterize the well-known LMMSE channel estimator. We first derive an asymptotic CME formulation that holds for a wide range of priors on the channel parameters. Based on this, we show that parametric Bayesian channel estimation is MSE-optimal for high signal-to-noise ratio (SNR) and/or long coherence intervals, i.e., many noisy observations provided within one coherence interval. Numerical simulations validate the derived formulations.

**Index Terms**—Channel estimation, parameter estimation, conditional mean estimation, mean square error, Cramer-Rao bound

## I. INTRODUCTION

ACCURATE channel estimation is a critical, long-standing issue in wireless communications systems. From classical estimation theory, it is well-understood that the conditional mean estimator (CME) is the optimal estimator in terms of mean square error (MSE) and all other Bregman loss functions [1]. Thus, many works have been dedicated to analyzing the CME and approximations thereof, e.g., [2]–[5]. As the CME needs access to the true underlying distribution, this distribution is estimated (implicitly or explicitly) based on a representative data set using machine learning.

In contrast to stochastic models, parametric channel estimators leverage the channel’s structural properties for estimation. In recent years, several such estimators have been proposed for millimeter wave (mmWave) systems, e.g., [6]–[10], as the assumption of sparse channels is valid for high frequencies. These techniques use unbiased estimators for the channel parameters and directly construct the channel accordingly. Additionally, parameter and parametric channel estimation become more relevant with the proposal of joint communication and sensing (JCAS) systems, as other system functionalities either provide or need the parameter information. A comprehensive overview of parametric channel estimation techniques for mmWave systems can be found in [9].

Naturally, the question arises if parametric channel estimation can achieve the minimum MSE (MSE). It is shown in [6], [7] that direction-of-arrival (DoA)-based channel estimation can achieve superior performance compared to an

approximate linear minimum MSE (MSE) estimator, which leverages estimates of the second order statistics based on the observations. The authors in [8] derive bounds based on the Cramer-Rao bound (CRB) of the error covariance matrix, which serve as a lower bound for unbiased parametric channel estimators. As the CME is not an unbiased estimator and is conceptually capable of extending the maximum-likelihood estimation principle, solely focusing on the CRB analysis is generally not optimal as the MMSE may lie below the CRB.

**Contributions:** We derive an expression of the CME for high signal-to-noise ratio (SNR) and/or long coherence intervals. We show that in this regime the CME does not utilize prior distribution knowledge but solely works with the current observation. Based on the Bayesian approach, we introduce a parametric channel estimator that achieves this MMSE in the asymptotic region, enabling MSE-optimal channel estimates without knowledge of the underlying channel or channel parameter distribution. Lastly, rigorous simulations show the validity of the derived bounds in the asymptotic region.

## II. PRELIMINARIES

### A. System Model

In time-varying multiple-input-multiple-output (MIMO) systems with multiple subcarriers, such as typical orthogonal frequency division multiplexing (OFDM) systems, the base-band model of resource block  $t$  can be described by

$$\mathcal{Y}(t) = \mathcal{H}(t) + \mathcal{N}(t) \in \mathbb{C}^{N_f \times N_t \times N_R \times N_T}, \quad (1)$$

where  $\mathcal{H}(t)$  and  $\mathcal{N}(t)$  are tensors denoting the channel and the additive white Gaussian noise and  $N_f$ ,  $N_t$ ,  $N_R$ , and  $N_T$  denote the number of subcarriers, symbols, receive and transmit antennas, respectively. The system model given in (1) can equivalently be described in its vectorized form as

$$\mathbf{y}(t) = \text{vec}(\mathcal{Y}(t)) = \mathbf{h}(t) + \mathbf{n}(t), \quad (2)$$

with  $\mathbf{y}(t) \in \mathbb{C}^{N_f N_t N_R N_T}$  and  $\mathbf{n}(t) \sim \mathcal{N}_{\mathbb{C}}(\mathbf{0}, \sigma^2 \mathbf{I})$ . The geometric channel model consisting of  $L$  paths is given as

$$\mathbf{h}(t) = \sum_{\ell}^L \alpha_{\ell}(t) \mathbf{a}_f(\tau_{\ell}) \otimes \mathbf{a}_t(\nu_{\ell}) \otimes \mathbf{a}_R(\theta_{\ell}) \otimes \mathbf{a}_T(\phi_{\ell}), \quad (3)$$

where  $\otimes$  denotes the Kronecker product and  $\alpha_{\ell}(t)$ ,  $\tau_{\ell}$ ,  $\nu_{\ell}$ ,  $\theta_{\ell}$ , and  $\phi_{\ell}$  denote the complex path loss, delay, Doppler-shift, DoA, and direction-of-departure (DoD) of the  $\ell$ -th path, respectively. We assume constant parameters within a coherence interval  $T$ , i.e., constant over  $T/N_t$  blocks, where only  $\alpha_{\ell}(t)$  depends on the block index  $t \in \{1, \dots, T/N_t\}$ . Further, the

This work was supported by the Federal Ministry of Research, Technology and Space of Germany in the programme of “Souverän. Digital. Vernetzt.”. Joint project 6G-life, project identification number: 16KISK002.

The authors are with the TUM School of Computation, Information and Technology, Technical University of Munich, 80333 Munich, Germany (e-mail: franz.weisser@tum.de).

path gain  $\alpha_\ell(t)$  is assumed to be invariant within one block. The generalized steering vector, which samples equidistantly in each of the respective domains, is defined as

$$\mathbf{a}_\xi(\omega_\ell^\xi) = \frac{1}{\sqrt{N_\xi}} [1, e^{-j\omega_\ell^\xi}, \dots, e^{-j(N_\xi-1)\omega_\ell^\xi}]^T, \quad (4)$$

where  $\xi \in \{f, t, R, T\}$  and  $\omega_\ell^\xi$  depends on  $\tau_\ell$ ,  $\nu_\ell$ ,  $\theta_\ell$ , and  $\phi_\ell$ , respectively. This work assumes  $N_f = N_t = N_T = 1$ , as the results can be straightforwardly extended. Hence, we use  $\mathbf{a}(\omega_\ell) = \mathbf{a}_R(\pi \sin(\theta_\ell))$  as a shortened notation. Further, we assume i.i.d. path gains with  $\alpha_\ell(n) \sim \mathcal{N}_C(0, \rho_\ell)$ <sup>1</sup> and  $\sum_{\ell=1}^L \rho_\ell = N_R$ , which leads to the SNR defined as  $\sigma^{-2}$ .

### B. Channel Estimation

We want to estimate the channel  $\mathbf{h}(T)$  given all observations  $\mathbf{Y} = [\mathbf{y}(1), \dots, \mathbf{y}(T)]$ , where we drop the index of  $\mathbf{h}(T)$  due to notational brevity. We consider the MSE as our optimality criterion, which is most frequently used and defined as

$$\text{MSE} = \mathbb{E} \left[ \|\mathbf{h} - \hat{\mathbf{h}}\|_2^2 \right], \quad (5)$$

where  $\hat{\mathbf{h}}$  denotes the estimate of  $\mathbf{h}$ .

### III. ASYMPTOTIC REGION ANALYSIS

In our work, the *asymptotic region* is the region of high SNR and/or long coherence intervals  $T$ . For our derivations, we approximate the inner product between steering vectors, for small enough  $\Delta\omega$ , by [7]

$$|\mathbf{a}^H(\omega)\mathbf{a}(\omega + \Delta\omega)|^2 \approx 1 - \frac{N_R^2(\Delta\omega)^2}{12}, \quad (6)$$

where the Taylor expansion is used, and any higher-order terms are neglected.

#### A. MMSE Channel Estimation

The optimal solution in terms of MSE is known to be the CME defined as [3]

$$\hat{\mathbf{h}}_{\text{CME}}(\mathbf{Y}) = \mathbb{E}[\mathbf{h} | \mathbf{Y}] = \mathbb{E}[\mathbb{E}[\mathbf{h} | \mathbf{Y}, \boldsymbol{\delta}] | \mathbf{Y}] \quad (7)$$

where the last equality follows from the law of total expectation for any latent variable  $\boldsymbol{\delta}$ . We introduce without loss of generality (w.l.o.g.)  $\boldsymbol{\delta} = [\omega, \rho]$  resulting in  $\mathbf{h} | \boldsymbol{\delta}$  being conditionally Gaussian distributed with zero mean, cf. [11]. The inner expectation of (7) results in the LMMSE estimator

$$\mathbb{E}[\mathbf{h} | \mathbf{Y}, \boldsymbol{\delta}] = \mathbf{W}_\delta \mathbf{y} = \mathbf{C}_{h|\delta} (\mathbf{C}_{h|\delta} + \mathbf{C}_n)^{-1} \mathbf{y}. \quad (8)$$

The CME, given  $\mathbf{Y}$ , can be calculated as [3]

$$\begin{aligned} \hat{\mathbf{h}}_{\text{CME}}(\mathbf{Y}) &= \mathbb{E}[\mathbf{W}_\delta | \mathbf{Y}] \mathbf{y} = \mathbf{W}_{\text{CME}}(\mathbf{Y}) \mathbf{y} \\ &= \frac{\int \exp \left( \frac{T}{\sigma^2} \text{tr}(\mathbf{W}_\delta \hat{\mathbf{C}}_y) + T \log |\mathbf{I} - \mathbf{W}_\delta| \right) \mathbf{W}_\delta p(\boldsymbol{\delta}) d\boldsymbol{\delta}}{\int \exp \left( \frac{T}{\sigma^2} \text{tr}(\mathbf{W}_\delta \hat{\mathbf{C}}_y) + T \log |\mathbf{I} - \mathbf{W}_\delta| \right) p(\boldsymbol{\delta}) d\boldsymbol{\delta}} \mathbf{y}, \end{aligned} \quad (9)$$

<sup>1</sup>For  $N_t > 1$ , the assumption of i.i.d. Gaussian path gains is an approximation as the steering vector  $\mathbf{a}_t(\cdot)$  models the phase evolution over time.

with  $\hat{\mathbf{C}}_y = \frac{1}{T} \mathbf{Y} \mathbf{Y}^H$ , and  $\mathbf{W}_\delta$  and  $p(\boldsymbol{\delta})$  denoting the conditional LMMSE filter as given in (8) and the prior distribution of  $\boldsymbol{\delta}$ . This CME can generally not be evaluated as the underlying distribution  $p(\boldsymbol{\delta})$  is unknown and the integral is intractable.

For our asymptotic analysis of the CME, we introduce the following lemma.

**Lemma 1.** *For a prior  $p(\boldsymbol{\delta})$  that is continuous on its support, let  $\mathbb{S} \subset \text{supp}(p(\boldsymbol{\delta}))$  be a connected subset of its support. Further let us denote with  $\text{diam}(\mathbb{S}) = \sup\{\|\boldsymbol{\delta}_1 - \boldsymbol{\delta}_2\| \mid \boldsymbol{\delta}_1, \boldsymbol{\delta}_2 \in \mathbb{S}\}$  the diameter of the set  $\mathbb{S}$ . A prior  $p(\boldsymbol{\delta})$  that satisfies*

$$\sup_{\boldsymbol{\delta} \in \mathbb{S}} \left| \frac{\partial p(\boldsymbol{\delta})}{\partial \boldsymbol{\delta}} \frac{1}{p(\boldsymbol{\delta})} \right| \ll \frac{1}{\text{diam}(\mathbb{S})} \quad (10)$$

is approximately constant over the set  $\mathbb{S}$ .

*Proof.* See Appendix A in the supplementary material.  $\square$

1) *Single-Path:* In the special case of  $L = 1$  the latent is  $\boldsymbol{\delta} = [\omega]$  resulting in the conditional LMMSE-filter as

$$\mathbf{W}_\delta = \frac{N_R}{N_R + \sigma^2} \mathbf{a}_\delta \mathbf{a}_\delta^H, \quad (11)$$

where  $\mathbf{a}_\delta = \mathbf{a}(\omega)$  leading to the following theorem.

**Theorem 1.** *Then, in the asymptotic region the CME filter in (9) for the considered system with  $L = 1$  is*

$$\mathbf{W}_{\text{CME}}(\mathbf{Y}) = \frac{1}{\sqrt{2\pi C}} \int \exp \left( -\frac{(\delta - \hat{\omega})^2}{2C} \right) \mathbf{W}_\delta d\delta, \quad (12)$$

with  $C = \frac{6\sigma^2(N_R + \sigma^2)}{TN_R^3 \bar{\alpha}}$ ,  $\bar{\alpha} = \frac{1}{T} \sum_{n=1}^T |\alpha(t)|^2$ .

*Proof.* See Appendix B in the supplementary material.  $\square$

We see in Theorem 1 that in the asymptotic region, the CME does not depend on the prior  $p(\boldsymbol{\delta})$  but solely on the Bartlett beamformer estimate  $\hat{\omega}$  [12]. Additionally, in the asymptotic region, i.e.,  $C \rightarrow 0$ , there exists a  $k$  for every continuous prior such that Lemma 1 is fulfilled.

2) *Multiple Paths:* In the case of  $L > 1$ , the parameter vector consists of  $\boldsymbol{\delta} = [\omega, \rho] = [\omega_1, \dots, \omega_L, \rho_1, \dots, \rho_L]$  and the integral in (9) becomes  $2L$  dimensional. The conditional channel covariance of  $\mathbf{h} | \boldsymbol{\delta}$  is given as

$$\mathbf{C}_{h|\delta} = \mathbf{A} \mathbf{C}_\rho \mathbf{A}^H, \quad (13)$$

with  $\mathbf{A} = [\mathbf{a}(\omega_1), \dots, \mathbf{a}(\omega_L)]$  and  $\mathbf{C}_\rho = \text{diag}(\rho_1, \dots, \rho_L) \in \mathbb{C}^{L \times L}$ . For large enough arrays, we assume favorable propagation, cf. [13, Chap. 2.5.2], rendering the LMMSE filter to

$$\mathbf{W}_\delta = \mathbf{A} \mathbf{C}_\rho (\mathbf{C}_\rho + \sigma^2 \mathbf{I})^{-1} \mathbf{A}^H \quad (14)$$

$$= \sum_{\ell=1}^L \frac{\rho_\ell}{\rho_\ell + \sigma^2} \mathbf{a}(\omega_\ell) \mathbf{a}^H(\omega_\ell), \quad (15)$$

which is a sum of  $L$  filters along the different directions.

In order to make the high SNR analysis feasible, we assume perfect knowledge of the individual path gains. This assumption can be motivated by the fact that empirical results show no significant dependency on the estimated path gains once a certain estimation quality is available.

**Corollary 1.** If Lemma 1 holds for  $\mathbb{S} = [\hat{\omega}_1 - k_1, \hat{\omega}_1 + k_1] \times \dots \times [\hat{\omega}_L - k_L, \hat{\omega}_L + k_L]$ , based on (15) and perfect path gain knowledge, the CME filter is

$$\mathbf{W}_{\text{CME}}(\mathbf{Y}) = \sum_{\ell=1}^L \frac{1}{\sqrt{2\pi C_\ell}} \frac{\rho_\ell}{\rho_\ell + \sigma^2} \int \exp\left(-\frac{(\delta - \hat{\omega}_\ell)^2}{2C_\ell}\right) \mathbf{a}_\delta \mathbf{a}_\delta^H d\delta, \quad (16)$$

with  $C_\ell = \frac{6\sigma^2(\rho_\ell + \sigma^2)}{TN_R^2 \rho_\ell \bar{\alpha}_\ell}$ ,  $\bar{\alpha}_\ell = \frac{1}{T} \sum_{n=1}^T |\alpha_\ell(t)|^2$  and  $\hat{\omega}_\ell$  denoting the Bartlett estimates of  $\omega_\ell$ .

*Proof.* Based on the decomposition in (15), the result follows from Theorem 1 for each direction separately.  $\square$

As in Theorem 1, the prior  $p(\delta)$  does not appear in (16) if the given conditions hold, particularly also if the individual  $\omega_\ell$  statistically depend on each other.

### B. Parametric Bayesian Channel Estimation

The CME in Theorem 1 and Corollary 1 solely relies on the parameter estimates  $\hat{\delta} = [\hat{\omega}, \hat{\rho}]$ . Similarly, in parametric channel estimation, these parameters are estimated as an intermediate step. Commonly, these estimates are used to directly build a channel estimate, e.g., [10]. On the contrary, the conditional Gaussian property of  $\mathbf{h} | \delta$  can be utilized, as done by the CME, to parameterize the LMMSE as

$$\hat{\mathbf{h}}_{\text{PBCE}}(\mathbf{Y}) = \mathbb{E}[\mathbf{h} | \mathbf{Y}, \hat{\delta}] = \mathbf{W}_{\hat{\delta}} \mathbf{y}, \quad (17)$$

which we refer to as the parametric Bayesian channel estimator (PBCE). This estimator does not utilize any prior distribution of  $\delta$ , and uses the maximum a-posteriori estimate of the filter  $\mathbf{W}_{\hat{\delta}}$  instead of solving the CME integral, by considering only the integrand with the highest probability. Independent of the used parameter estimator, the PBCE is generally biased, hence, a comparison to the CME is more applicable than to the CRB.

**Theorem 2.** The difference between the asymptotic bounds (ABs) of the CME and the PBCE vanishes quadratically with the noise variance as

$$\lim_{\sigma^2 \rightarrow 0} \frac{\log(\text{CME}^{\text{AB}} - \text{PBCE}^{\text{AB}})}{\log \sigma^2} = 2. \quad (18)$$

*Proof.* The AB of the CME is shown in (19) at the bottom of the page with  $B = \frac{N_R^2}{24}$  and  $\bar{C}_\ell = \mathbb{E}[C_\ell]$ . The calculations for the single-path case are sketched in Appendix C in the supplementary material, which can be easily extended to the multi-path case. The AB of the PBCE can be found similarly,

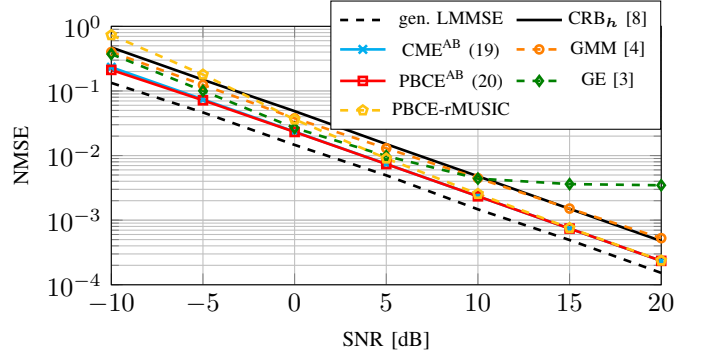


Fig. 1. NMSE over the SNR in the  $L = 1$  path and  $N_R = 64$  antenna scenario based on  $T = 1$  observations.

resulting in (20), also shown at the bottom of the page. The limit in (18) follows from (19) and (20).  $\square$

In the case of  $T \rightarrow \infty$  the bounds converge linearly to each other. Both MSE formulations depend on the parameter's CRB as the CME and the PBCE use (or are assumed to use) an unbiased parameter estimator. If a parameter estimator is chosen for the PBCE, which converges faster to the CRB than the Bartlett beamformer, cf. [14], the PBCE converges faster to its asymptote than the CME.<sup>2</sup>

### IV. NUMERICAL SIMULATIONS

We validate the derived bounds using the normalized MSE (MSE) defined as  $\frac{1}{N_R} \text{MSE}$ , which we approximate by  $M = 10^3$  Monte-Carlo simulations. If not stated otherwise, we use  $N_R = 64$  antennas. For the prior distribution, we use 4 regions, where each region can be described by a Gaussian probability density function (PDF) with  $\mu_i \in \{-70^\circ, -30^\circ, 20^\circ, 60^\circ\}$  and  $\sigma_i \in \{5^\circ, 10^\circ, 5^\circ, 10^\circ\}$ , respectively. The probability that the channel corresponds to a certain region is  $p_i \in \{0.1, 0.5, 0.2, 0.2\}$ , and all path angles are drawn from the same Gaussian PDF.<sup>3</sup> Additionally, we uniformly sample  $\rho_\ell \sim \mathcal{U}[0, N_R]$  and normalize it such that  $\sum_{\ell=1}^L \rho_\ell = N_R$ .

For the PBCE, we use root multiple signal classification (rMUSIC) [15] to estimate the  $L$  DoAs, as rMUSIC does not suffer from the grid mismatch problem and is shown to be asymptotically efficient. We estimate the path gains with [16]

$$\hat{\rho} = \text{diag}\left((\hat{\mathbf{A}}^H \hat{\mathbf{A}})^{-1} \hat{\mathbf{A}}^H (\hat{\mathbf{C}}_{\mathbf{y}} - \sigma^2 \mathbf{I}) \hat{\mathbf{A}} (\hat{\mathbf{A}}^H \hat{\mathbf{A}})^{-1}\right), \quad (21)$$

<sup>2</sup>One should note that for  $L > 1$  standard DoA estimators are only asymptotically efficient for high  $T$ , not high SNR.

<sup>3</sup>The quantitative results of the simulations are the same for any prior satisfying Lemma 1.

$$\text{CME}^{\text{AB}} = N_R - 2 \sum_{\ell=1}^L \left( \frac{\rho_\ell}{\rho_\ell + \sigma^2} \right) (\rho_\ell (1 - 2B\bar{C}_\ell) - 2B \text{CRB}_\omega) + \sum_{\ell=1}^L \left( \frac{\rho_\ell}{\rho_\ell + \sigma^2} \right)^2 (\rho_\ell (1 - 4B\bar{C}_\ell) - 2B \text{CRB}_\omega + \sigma^2) \quad (19)$$

$$\text{PBCE}^{\text{AB}} = N_R - 2 \sum_{\ell=1}^L \left( \frac{\rho_\ell}{\rho_\ell + \sigma^2} \right) (\rho_\ell - 2B \text{CRB}_\omega) + \sum_{\ell=1}^L \left( \frac{\rho_\ell}{\rho_\ell + \sigma^2} \right)^2 (\rho_\ell - 2B \text{CRB}_\omega + \sigma^2) \quad (20)$$

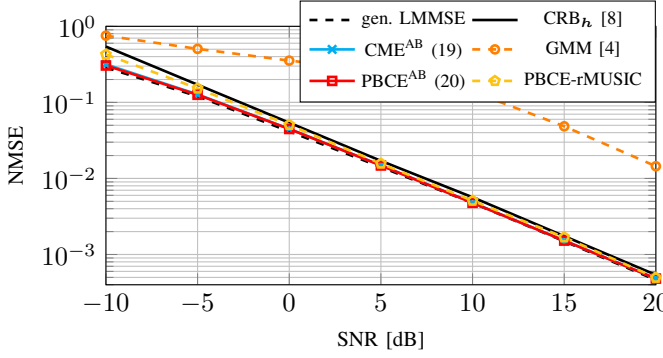


Fig. 2. NMSE over the SNR in the  $L = 3$  path and  $N_R = 64$  antenna scenario based on  $T = 16$  observations.

where  $\hat{\mathbf{A}} = [\mathbf{a}(\hat{\omega}_1), \dots, \mathbf{a}(\hat{\omega}_L)]$  holds the steering vectors based on the parameter estimates.

We also compare to the channel estimator from [4], which does not use structural information (i.e., it is non-parametric) and approximates the CME by learning a Gaussian mixture model (GMM) representation of the underlying channel distribution. In the single-path case, we evaluate the gridded estimator (GE) introduced in [3], which uses a sampled version of the true channel distribution, making the integral in (9) feasible to calculate. Lastly, the utopian genie-aided LMMSE estimator is simulated with

$\hat{\mathbf{h}}_{\text{gen. LMMSE}}(\mathbf{Y}, \delta) = \mathbb{E}[\mathbf{h} | \mathbf{Y}, \delta] = \mathbf{W}_\delta \mathbf{y}$ , which uses perfect knowledge of the channel parameters.

#### A. Single-Path

Fig. 1 shows the channel estimation results based on  $T = 1$  observations for  $L = 1$  based on different SNR values. We can directly see that the “CRB<sub>h</sub>” from [8], which is the lower bound for unbiased channel estimators, is outperformed by the Bayesian-based estimators. We see that the PBCE based on rMUSIC converges for high SNR values to the derived bounds of the CME (19) and PBCE (20). This convergence validates the derived MSEs formulations. Additionally, we observe that in the low SNR region, the PBCE degrades in performance compared to the GMM and the GE. This decline is primarily because the PBCE fully trusts its parameter estimates (which become worse for low SNR) and does not take noise-dependent uncertainties into account. For higher SNR values, the GMM-based CME approximation shows inferior performance compared to PBCE. Furthermore, we see that for high SNR, the GE becomes victim to the grid mismatch problem, saturating for SNR values above 10dB. Interestingly, the CME does not coincide with the genie-aided LMMSE even for high SNR, which shows that achieving the MMSE is possible without perfect channel parameter knowledge.

#### B. Multiple Paths

For the rest of the simulations, we assume channels with  $L = 3$  paths, where the number of paths is assumed to be known at the receiver.<sup>4</sup> In Fig. 2, the NMSE performance

<sup>4</sup>This assumption is reasonable as good model order selection can be achieved for high SNR and/or a high number of snapshots, cf. [17].

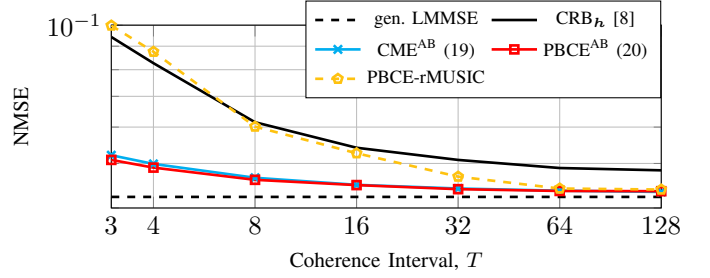


Fig. 3. NMSE over the length of the coherence interval  $T$  at SNR = 0dB in the  $L = 3$  path and  $N_R = 64$  antennas scenario.

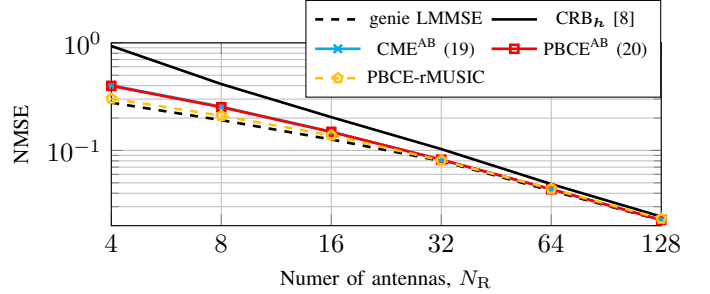


Fig. 4. NMSE over number of antennas at SNR = 0dB and  $T = 64$  in the  $L = 3$  path scenario.

is shown for  $T = 16$  observations to ensure asymptotic performance of rMUSIC. Again, the two derived MSE formulations in (19) and (20) show the best NMSE, which are only surpassed by the genie-aided LMMSE. One should note that in the multi-path setup, the derived MSE formulation (19) and (20) do not represent an asymptotic MSE formulation but rather give a lower bound on the asymptotic MSE as we assumed perfect path gain knowledge during the derivations.

As the asymptotic efficiency of rMUSIC holds for large  $T$ , Fig. 3 shows the performance for SNR= 0dB over the length of the coherence interval  $T$ . As expected, the performance decreases for all estimators approaching the CME bound (19), validating the latter.

The last simulations in Fig. 4 show the performance over different numbers of antennas in the asymptotic region at  $T = 64$  and SNR= 0dB. First, we realize that for low numbers of antennas, the PBCE using rMUSIC outperforms our derived bounds. In this region, the assumption of favorable propagation no longer holds, making our bounds invalid. Additionally, we see that for large  $N_R$ , the gap between the “CRB<sub>h</sub>” and the CME formulation narrows.

## V. CONCLUSION

In this work, we derived a CME formulation for high SNR and/or long coherence intervals in mmWave systems, which holds for distributions on the channel parameters that fulfill a specific criterion on the slope of their PDF. Based on this formulation, we showed that PBCE can achieve this MSE-optimal performance in the asymptotic region. Numerical simulations validate that PBCE converges to the derived bounds, making it a superior channel estimation framework to unbiased parametric channel estimation.

## REFERENCES

- [1] A. Banerjee, X. Guo, and H. Wang, "On the optimality of conditional expectation as a Bregman predictor," *IEEE Transactions on Information Theory*, vol. 51, no. 7, pp. 2664–2669, 2005.
- [2] D. Guo, Y. Wu, S. S. Shitz, and S. Verdú, "Estimation in gaussian noise: Properties of the minimum mean-square error," *IEEE Transactions on Information Theory*, vol. 57, no. 4, pp. 2371–2385, 2011.
- [3] D. Neumann, T. Wiese, and W. Utschick, "Learning the MMSE channel estimator," *IEEE Transactions on Signal Processing*, vol. 66, no. 11, pp. 2905–2917, 2018.
- [4] M. Koller, B. Fesl, N. Turan, and W. Utschick, "An asymptotically MSE-optimal estimator based on Gaussian mixture models," *IEEE Transactions on Signal Processing*, vol. 70, pp. 4109–4123, 2022.
- [5] F. Weißer, N. Turan, and W. Utschick, "DoA-aided MMSE channel estimation for wireless communication systems," in *ICASSP 2025 - 2025 IEEE International Conference on Acoustics, Speech and Signal Processing (ICASSP)*, 2025.
- [6] B. Yang, K. Letaief, R. Cheng, and Z. Cao, "Channel estimation for OFDM transmission in multipath fading channels based on parametric channel modeling," *IEEE Transactions on Communications*, vol. 49, no. 3, pp. 467–479, 2001.
- [7] R. Shafin, L. Liu, J. Zhang, and Y.-C. Wu, "DoA estimation and capacity analysis for 3-d millimeter wave massive-MIMO/FD-MIMO OFDM systems," *IEEE Transactions on Wireless Communications*, vol. 15, no. 10, pp. 6963–6978, 2016.
- [8] M. D. Larsen, A. L. Swindlehurst, and T. Svanesson, "Performance bounds for MIMO-OFDM channel estimation," *IEEE Transactions on Signal Processing*, vol. 57, no. 5, pp. 1901–1916, 2009.
- [9] K. Hassan, M. Masarra, M. Zwingelstein, and I. Dayoub, "Channel estimation techniques for millimeter-wave communication systems: Achievements and challenges," *IEEE Open Journal of the Communications Society*, vol. 1, pp. 1336–1363, 2020.
- [10] J. Zhang, D. Rakhimov, and M. Haardt, "Gridless channel estimation for hybrid MmWave MIMO systems via tensor-ESPRIT algorithms in DFT beamspace," *IEEE Journal of Selected Topics in Signal Processing*, vol. PP, pp. 1–1, 03 2021.
- [11] B. Böck, M. Baur, N. Turan, D. Semmler, and W. Utschick, "A statistical characterization of wireless channels conditioned on side information," *IEEE Wireless Communications Letters*, pp. 1–1, 2024.
- [12] M. S. Bartlett, "Periodogram analysis and continuous spectra," *Biometrika*, vol. 37, no. 1/2, pp. 1–16, 1950.
- [13] E. Björnson, J. Hoydis, and L. Sanguinetti, "Massive MIMO networks: Spectral, energy, and hardware efficiency," *Foundations and Trends® in Signal Processing*, vol. 11, no. 3-4, pp. 154–655, 2017. [Online]. Available: <http://dx.doi.org/10.1561/20000000093>
- [14] H. Gazzah and J.-P. Delmas, "Spectral efficiency of beamforming-based parameter estimation in the single source case," in *2011 IEEE Statistical Signal Processing Workshop (SSP)*, 2011, pp. 153–156.
- [15] A. Barabell, "Improving the resolution performance of eigenstructure-based direction-finding algorithms," in *ICASSP '83. IEEE International Conference on Acoustics, Speech, and Signal Processing*, vol. 8, 1983, pp. 336–339.
- [16] R. Schmidt, "Multiple emitter location and signal parameter estimation," *IEEE Transactions on Antennas and Propagation*, vol. 34, no. 3, pp. 276–280, 1986.
- [17] M. Wax and T. Kailath, "Detection of signals by information theoretic criteria," *IEEE Transactions on Acoustics, Speech, and Signal Processing*, vol. 33, no. 2, pp. 387–392, 1985.

## APPENDIX

## A. Proof of Lemma 1

If the constraint (10) is fulfilled, based on the mean value theorem for two arbitrary points  $\delta_1, \delta_2 \in \mathbb{S}$  there exists a  $\delta \in \mathbb{S} \setminus \partial\mathbb{S}$  such that

$$\left| \frac{p(\delta_1) - p(\delta_2)}{(\delta_1 - \delta_2)p(\delta_2)} \right| = \left| \frac{\partial p(\delta)}{\partial \delta} \frac{1}{p(\delta)} \right| \ll \frac{1}{\text{diam}(\mathbb{S})}. \quad (22)$$

In the case of  $p(\delta_1) \geq p(\delta_2)$  we have

$$1 \leq \frac{p(\delta_1)}{p(\delta_2)} \ll 1 + \frac{|\delta_1 - \delta_2|}{\text{diam}(\mathbb{S})} \leq 2, \quad (23)$$

and for  $p(\delta_1) < p(\delta_2)$  we have

$$1 > \frac{p(\delta_1)}{p(\delta_2)} \gg 1 - \frac{|\delta_1 - \delta_2|}{\text{diam}(\mathbb{S})} \geq 0, \quad (24)$$

from which we can conclude  $p(\delta_1) \approx p(\delta_2) \forall \delta_1, \delta_2 \in \mathbb{S}$ .  $\square$

## B. Proof of Theorem 1

The term  $T \log |\mathbf{I} - \mathbf{W}_\delta|$  in (9) is independent of  $\delta$  and, hence, the resulting optimal CME filter, given  $\mathbf{Y}$ , is

$$\mathbf{W}_{\text{CME}}(\mathbf{Y}) = \frac{\int \exp\left(\frac{TN_R}{\sigma^2(N_R + \sigma^2)} \mathbf{a}_\delta^H \hat{\mathbf{C}}_y \mathbf{a}_\delta\right) \mathbf{W}_\delta p(\delta) d\delta}{\int \exp\left(\frac{TN_R}{\sigma^2(N_R + \sigma^2)} \mathbf{a}_\delta^H \hat{\mathbf{C}}_y \mathbf{a}_\delta\right) p(\delta) d\delta}. \quad (25)$$

The argument of the exponential function in (25) resembles the Bartlett beamformer [12]. In the asymptotic region, the Bartlett spectrum exhibits one distinct peak, which we approximate around its maximum value  $\hat{\omega}$  using (6) as

$$\mathbf{a}_\delta^H \hat{\mathbf{C}}_y \mathbf{a}_\delta \approx \bar{\alpha} |\mathbf{a}_\delta^H \mathbf{a}(\hat{\omega})|^2 \approx \bar{\alpha} \left(1 - \frac{N_R^2(\delta - \hat{\omega})^2}{12}\right), \quad (26)$$

which approaches equality for small  $\delta - \hat{\omega}$ . The needed exponential function of (25) can therefore be written as

$$\begin{aligned} & \exp\left(\frac{TN_R}{\sigma^2(N_R + \sigma^2)} \mathbf{a}_\delta^H \hat{\mathbf{C}}_y \mathbf{a}_\delta\right) \\ &= \exp\left(\frac{TN_R \bar{\alpha}}{\sigma^2(N_R + \sigma^2)}\right) \exp\left(-\frac{(\delta - \hat{\omega})^2}{2C}\right). \end{aligned} \quad (27)$$

Furthermore, we realize that the exponential function is proportional to a Gaussian PDF with variance  $C$ . Based on the Chernoff bound, the integral of the tails can be bounded as

$$\int_{\hat{\omega}+k}^{\infty} \exp\left(-\frac{(\delta - \hat{\omega})^2}{2C}\right) d\delta \leq \sqrt{2\pi C} \exp\left(\frac{-k^2}{2C}\right), \quad (28)$$

respectively, which becomes negligible for large enough  $k$ . If now the prior  $p(\delta)$  satisfies Lemma 1 with  $\mathbb{S} = [\hat{\omega} - k, \hat{\omega} + k]$ , while  $k$  being large enough to neglect the tails, it is approximately constant in the contributing interval, and, hence, cancels out, which concludes the proof.  $\square$

## C. MSE Calculation for Single-Path

The MSE is given as

$$\begin{aligned} \mathbb{E}[\|\mathbf{h} - \hat{\mathbf{h}}\|^2] &= \mathbb{E}[\|\mathbf{h} - \mathbf{W}\mathbf{y}\|^2] \\ &= N_R - \mathbb{E}[2\mathbf{h}^H \mathbf{W}\mathbf{h}] + \mathbb{E}[\|\mathbf{W}\mathbf{h}\|^2] + \mathbb{E}[\|\mathbf{W}\mathbf{n}\|^2], \end{aligned} \quad (29)$$

where  $\mathbf{W}$  denotes the current filter of interest and  $\hat{\mathbf{h}} = \mathbf{W}\mathbf{y}$  is the estimate of  $\mathbf{h}$ . In the case of (12) we have

$$\begin{aligned} \mathbb{E}[\mathbf{h}^H \mathbf{W}\mathbf{h}] & \quad (30) \\ &= \mathbb{E}\left[\frac{1}{\sqrt{2\pi C}} \frac{N_R}{N_R + \sigma^2} \int \exp\left(-\frac{(\delta - \hat{\omega})^2}{2C}\right) |\mathbf{h}^H \mathbf{a}_\delta|^2 d\delta\right] \end{aligned} \quad (31)$$

$$= \frac{N_R}{N_R + \sigma^2} (N_R(1 - 2B\bar{C}) - 2B\mathbb{E}[|\alpha|^2(\Delta\omega)^2]), \quad (32)$$

with  $\bar{C} = \mathbb{E}[C]$ , where in the last step the approximation (6) is used. In [14] it has been proven that the Bartlett estimator is asymptotically unbiased and efficient in the single source case, hence, using the law of total expectation we have

$$\begin{aligned} \mathbb{E}[|\alpha|^2(\Delta\omega)^2] &= \mathbb{E}_\alpha \left[ |\alpha|^2 \mathbb{E}_{(\Delta\omega)^2|\alpha} [(\Delta\omega)^2 | \alpha] \right] \\ &= \frac{\sigma^2}{2T} [\Re\{\dot{\mathbf{a}}^H (\mathbf{I} - \mathbf{a}\mathbf{a}^H)^{-1} \dot{\mathbf{a}}\}]^{-1} = \text{CRB}_\omega, \end{aligned} \quad (33)$$

where  $\dot{\mathbf{a}} = \partial \mathbf{a}(\omega) / \partial \omega$ .

Similarly, for  $\mathbb{E}[\|\mathbf{W}\mathbf{h}\|^2]$  two integrals have to be evaluated as shown in (34) at the bottom of this page, where the following approximation can be used

$$\begin{aligned} & \Re\{\mathbf{h}^H \mathbf{a}_\delta \mathbf{a}_\delta^H \mathbf{a}_\zeta \mathbf{a}_\zeta^H \mathbf{h}\} \\ &= \frac{|\alpha|^2}{N_R^3} \frac{\sin\left(\frac{N_R(\delta - \omega)}{2}\right)}{\sin\left(\frac{\pi(\delta - \omega)}{2}\right)} \frac{\sin\left(\frac{N_R(\zeta - \delta)}{2}\right)}{\sin\left(\frac{\pi(\zeta - \delta)}{2}\right)} \frac{\sin\left(\frac{N_R(\omega - \zeta)}{2}\right)}{\sin\left(\frac{\pi(\omega - \zeta)}{2}\right)} \end{aligned} \quad (35)$$

$$\approx |\alpha|^2 (1 - B(\delta - \omega)^2 - B(\zeta - \delta)^2 - B(\omega - \zeta)^2), \quad (36)$$

which holds with equality for small differences between the angles.

## D. Visualization of the Prior Distribution

Fig. 5 shows the probability distribution of the angles for the four regions defined in Section IV. The multiple path angles of each channel realization are drawn from the same Gaussian PDF.

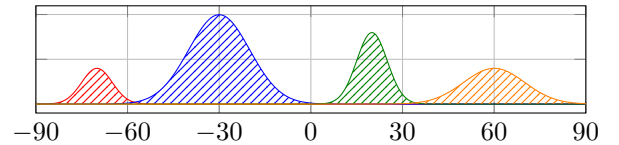


Fig. 5. Probability distribution of the path angles with four regions.

$$\mathbf{h}^H \mathbf{W}^H \mathbf{W} \mathbf{h} = \frac{1}{2\pi C} \left( \frac{N_R}{N_R + \sigma^2} \right)^2 \int \int \exp\left(-\frac{(\delta - \hat{\omega})^2}{2C}\right) \exp\left(-\frac{(\zeta - \hat{\omega})^2}{2C}\right) \mathbf{h}^H \mathbf{a}_\delta \mathbf{a}_\delta^H \mathbf{a}_\zeta \mathbf{a}_\zeta^H \mathbf{h} d\delta d\zeta. \quad (34)$$